

A novel auxiliary equation neural networks method for exactly explicit solutions of nonlinear partial differential equations

Shanhao Yuan^{a,b}, Yanqin Liu^{a,*}, Runfa Zhang^{c,d,*}, Limei Yan^a, Shunjun Wu^a, Libo Feng^e

^a*School of Mathematics and Big Data, Dezhou University, Dezhou 253023, China*

^b*School of Mathematics and Statistics, Qilu University of Technology (Shandong Academy of Sciences), Jinan 250353, China*

^c*School of Automation and Software Engineering, Shanxi University, Taiyuan 030013, China*

^d*Hubei Key Laboratory of Applied Mathematics, Hubei University, Wuhan 430062, China*

^e*School of Mathematical Sciences, Queensland University of Technology, GPO Box 2434, Brisbane, Qld. 4001, Australia*

Abstract

In this study, we firstly propose an auxiliary equation neural networks method (AENNM), an innovative analytical method that integrates neural networks (NNs) models with the auxiliary equation method to obtain exact solutions of nonlinear partial differential equations (NLPDEs). A key novelty of this method is the introduction of a novel activation function derived from the solutions of the Riccati equation, establishing a new mathematical link between differential equations theory and deep learning. By combining the strong approximation capability of NNs with the high precision of symbolic computation, AENNM significantly enhances computational efficiency and accuracy. To demonstrate the effectiveness of the AENNM in solving NLPDEs, three numerical examples are investigated, including the nonlinear evolution equation, the Korteweg-de Vries-Burgers equation, and the (2+1)-dimensional Boussinesq equation. Furthermore, some new trial functions are constructed by setting specific activation functions within the "2-2-2-1" and "3-2-2-1" NNs models. By embedding the auxiliary equation method into the NNs framework, we derive previously unreported solutions. The exact analytical solutions are expressed in terms of hyperbolic functions, trigonometric functions, and rational functions. Finally, three-dimensional plots, contour plots, and density plots are presented to illustrate the dynamic characteristics of the obtained solutions. This research provides a novel methodological framework for addressing NLPDEs, with broad applicability across scientific and engineering fields.

Keywords: Neural networks, Nonlinear partial differential equation, Auxiliary equation, Exact solution

1. Introduction

Nonlinear partial differential equations (NLPDEs) are important mathematical tools for describing complex natural phenomena and engineering problems. Unlike their linear

*Corresponding author.

Email addresses: yqliumath@163.com (Yanqin Liu), rf_zhang@sina.cn (Runfa Zhang)

counterparts, NLPDEs exhibit intricate behaviors such as blow-up, solitons, shock waves, and chaos [1–3], making them both challenging and essential for understanding real-world systems. Compared to numerical methods, analytical solutions not only reveal the intrinsic symmetries and conservation laws of a system but also serve as benchmark validations for numerical simulations. For instance, in optical fiber communications, the soliton solutions of the nonlinear Schrödinger equation provide the theoretical foundation for distortion-free pulse propagation [4], while the exact solutions of shallow water wave equations are critical for tsunami early-warning modeling [5]. Exploring exact solutions to NLPDEs has become a key focus in understanding various physical phenomena and continues to attract growing attention from researchers worldwide.

In the past several decades, many analytical methods have been established and developed. Within the integrability framework, Hirota’s bilinear method [6, 7] transforms the nonlinear equation into a bilinear form through variable substitution, thereby enabling the direct construction of soliton solutions. Complementary approaches like the Bäcklund transformation [8–10] establish differential constraints between solutions, providing a generative mechanism for exotic localized waves such as lump solitons. As a classical tool for integrable systems, the inverse scattering method [11–13] converts nonlinear problems into linear integral equations through spectral theory, and has been successfully applied to models such as the KdV equation. For traveling wave solutions, the Jacobi elliptic function method [14, 15], leverages periodicity to approximate solutions, though its efficacy depends on specific nonlinear term structures. The tanh-function expansion and its various extension [16–18], solves traveling wave solutions of nonlinear equations through polynomial combinations of hyperbolic tangent functions. The F-expansion method [19–21] further broadens applicability to higher dimensions through auxiliary ordinary differential equations. Notably, the (G'/G) -expansion method [22–24] parametrizes solution families using rational functions of solutions to linear ordinary differential equations, while the exp-function method [25–27] employs exponential terms to construct multi-peakon solutions, albeit requiring rigorous validation to exclude spurious solutions. However, the diversity of nonlinear terms in NLPDEs, including dispersion, dissipation, and convective effects, makes a universal analytical method unattainable.

With the emergence of artificial intelligence, deep learning is widely used in the fields of science and technology [28–30]. The universal approximation theorem states that a fully connected neural networks (NNs) can approximate any continuous function with arbitrary accuracy [31]. Raissi et al. [32] introduced physics-informed neural networks (PINNs), a class of machine learning models that embed physical laws directly into their training process to solve NLPDEs. Lu et al. [33] proposed deep operator network (DeepONet), a neural network with small generalization error for learning nonlinear operators by combining a branch net to encode the discrete input function space and a trunk net to encode domain of the output functions. Subsequently, Wang et al. [34] developed physics-informed DeepONet, which first employs DeepONet to learn the solution operator of PDEs, then utilizes this operator as prior knowledge in PINNs to accelerate the training process while achieving higher accuracy. Nevertheless, these NNs methods provide approximate solutions rather than exact solutions, inevitably introducing numerical errors. Being data-driven models, these techniques necessitate large-scale training data, which imposes significant computational overhead. Moreover, the performance of NNs

heavily depends on optimization algorithms for parameter tuning, which can be computationally intensive. Therefore, improving training efficiency and developing more robust optimization strategies remain critical research directions.

Recently, the integration of NNs with symbolic computation for quickly obtaining exact solutions to NLPDEs has attracted significant research attention. Zhang et al. [35] proposed the bilinear neural network method (BNNM), which combines the bilinear approach with NNs models to obtain exact solutions for NLPDEs. Subsequently, the bilinear residual network method [36] was developed to obtain exact explicit solutions for nonlinear evolution equations while reducing model complexity. Liu et al. [37] investigated a multivariate bilinear neural network method by improving the BNNM, introducing multivariate functions as activation functions in the NNs. Wu et al. [38] introduced a variable coefficient bilinear residual network method, which effectively addresses the issue of variable coefficients in nonlinear integrable systems with variable coefficients. Zhu et al. [39] derived the bilinear form of the fractional (3+1)-dimensional Yu-Toda-Sasa-Fukuyama equation by combining the Bell polynomial approach with NNs.

Inspired by the above works, an auxiliary equation neural networks method, which embeds the auxiliary equation method into the NNs architecture, is firstly proposed to solve NLPDEs in this paper. Our major contributions are highlighted as follows:

- We apply NNs architecture to construct the potential analytical solution of NLPDEs. The output of AENNM, obtained through feedforward computation comprising weights, biases and activation functions, serves as a trial function for the NLPDEs.
- A novel activation function derived from the solutions of the Riccati equation is creatively introduced for NNs, establishing a new mathematical connection between differential equations and deep learning.
- We provide an innovative method that utilizes NNs without data samples to obtain exact symbolic analytical solutions of NLPDEs. Thus, the computational efficiency and accuracy of NLPDEs are significantly improved.
- This approach employs NNs to systematize and clarify the construction of the trial function. The network structure introduced is both adaptable and configurable, allowing it to be tailored to diverse types of NLPDEs through modifications in the number of network layers, neurons, and types of activation functions.

The structure of this paper is as follows. In Section 2, we introduce the theory of the proposed method. In Section 3, the accuracy and feasibility of the analytical method for NLPDEs are verified through the nonlinear evolution equation, the Korteweg-de Vries-Burgers equation, and the (2+1)-dimensional Boussinesq equation. In Section 4, the proposed method is compared with existing method in the literature. Finally, the discussions and conclusions of this paper are given in Section 5 and Section 6, respectively.

2. Auxiliary equation neural networks method (AENNM)

In this section, we introduce the idea of the AENNM for finding solutions of NLPDEs. Consider the following general NLPDEs

$$\mathcal{L}\{u(x, t)\} + \mathcal{N}\{u(x, t)\} = 0, \quad (2.1)$$

where $u(x, t)$ is the solution of the equation, $\mathcal{L}\{u(x, t)\}$ is a linear operator that involves $u(x, t)$ and its various partial derivatives with respect to x and t , $\mathcal{N}\{u(x, t)\}$ is a nonlinear operator that encompasses $u(x, t)$ and its various partial derivatives.

The method uses the output of the NNs as a trial function to obtain the analytical solutions of the NLPDEs. We initially simplify the NLPDEs into a set of easily solvable nonlinear algebraic equations by applying the trial function. Subsequently, we determine the corresponding weights and biases of NNs by solving the system of nonlinear algebraic equations.

To obtain the solution $u(x, t)$ of the NLPDEs, we utilize a 2-2-2-1 model within the feedforward computation of the NNs, which has two hidden layers l_1 and l_2 , each consisting of two neurons, as shown in Fig. 1a. Thus, the mathematical mapping corresponding to the explicit model is as follows

$$\begin{cases} \xi_1 = tw_{t1} + xw_{x1} + b_1, \\ \xi_2 = tw_{t2} + xw_{x2} + b_2, \\ \xi_3 = w_{23}F_2(\xi_2) + w_{13}F_1(\xi_1) + b_3, \\ \xi_4 = w_{24}F_2(\xi_2) + w_{14}F_1(\xi_1) + b_4, \\ u(x, t) = w_{3u}F_3(\xi_3) + w_{4u}F_4(\xi_4) + b_5, \end{cases} \quad (2.2)$$

where ξ_1 and ξ_2 are the outputs of the first and second neurons in the first hidden layer respectively, ξ_3 and ξ_4 are the outputs of the first and second neurons in the second hidden layer respectively, w_{ij} ($i = t, x, 1, 2, 3, 4, j = 1, 2, 3, 4, u$) are the weights between the each neurons, F_1, F_2, F_3, F_4 are the activation functions, b_1, b_2, b_3, b_4, b_5 are the biases of each neurons. The trial function $u(x, t)$ of the Eq. (2.2) based on NNs architecture is composed of weights and biases.

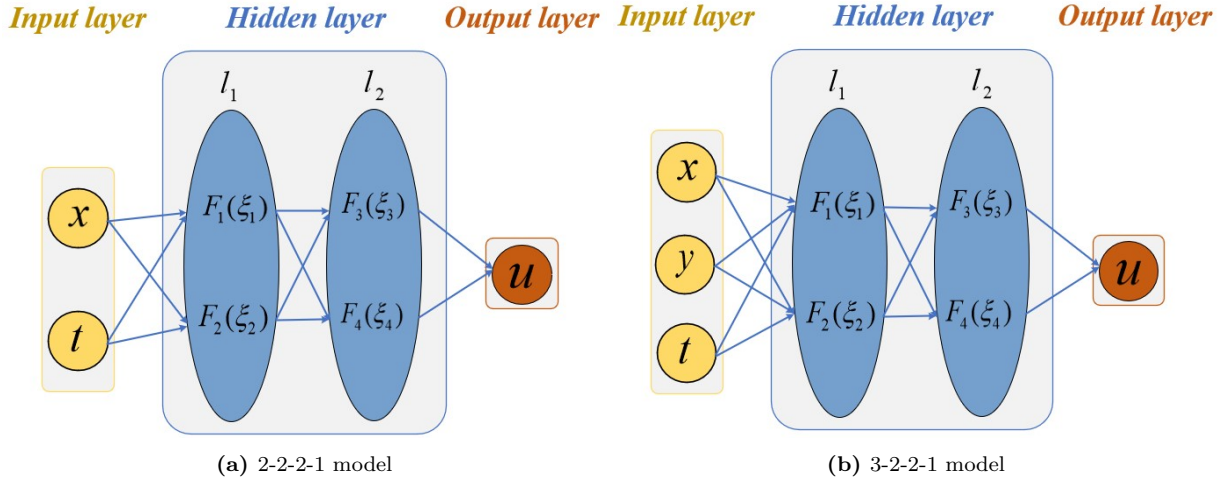


Fig. 1. NNs architectures for obtaining the exact analytical solutions of NLPDEs.

Unlike the 2-2-2-1 model, the 3-2-2-1 model has three inputs while keeping the rest of the networks structure unchanged, as shown in Fig. 1b. Thus, the trial function $u(x, y, t)$ is

$$\begin{cases} \xi_i = tw_{ti} + yw_{yi} + xw_{xi} + b_i, (i = 1, 2), \\ \xi_j = w_{2j}F_2(\xi_2) + w_{1j}F_1(\xi_1) + b_j, (j = 3, 4), \\ u(x, y, t) = w_{3u}F_3(\xi_3) + w_{4u}F_4(\xi_4) + b_5. \end{cases} \quad (2.3)$$

In this paper, a novel activation function

$$\varphi(\xi_i) = \begin{cases} -\sqrt{-b} \tanh \sqrt{-b} \xi_i, & b < 0, \\ -\sqrt{-b} \coth \sqrt{-b} \xi_i, & b < 0, \\ -\frac{1}{\xi_i}, & b = 0, \\ \sqrt{b} \tan \sqrt{b} \xi_i, & b > 0, \\ -\sqrt{b} \cot \sqrt{b} \xi_i, & b > 0, \end{cases} \quad (2.4)$$

derived from the solutions of the Riccati equation

$$\varphi' = b + \varphi^2, \quad (2.5)$$

is creatively introduced for NNs.

In the AENNM, if the activation functions F_1 and F_2 in the first hidden layer are specified as $\varphi(\cdot)$, the solution of the NLPDEs can be expressed as a polynomial of $\varphi(\cdot)$. The proposed method provides interpretable activation functions derived from the auxiliary equation, thereby eliminating the blindness in activation function selection. The AENNM merges the precision characteristic of symbolic computation with the adaptive capabilities inherent in NNs, substantially enhancing both computational efficiency and accuracy.

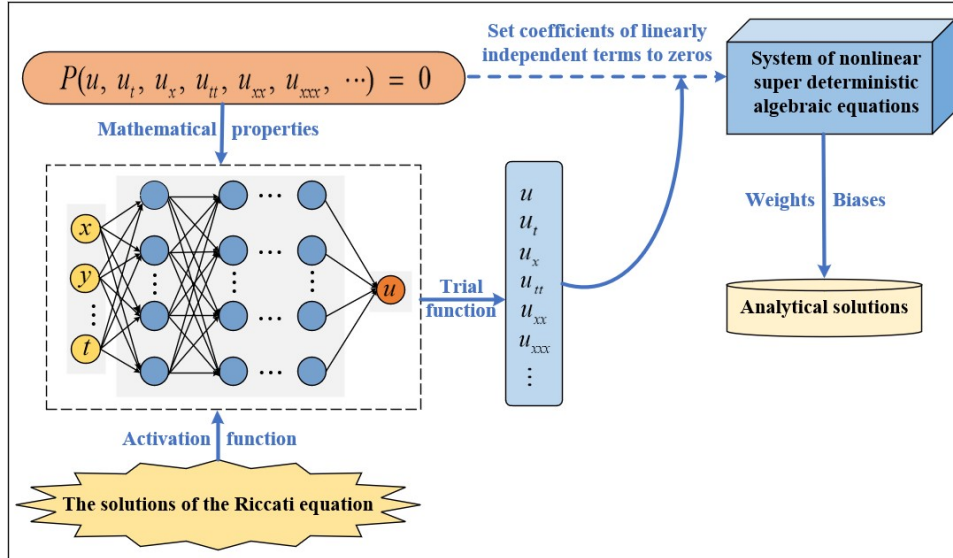


Fig. 2. The algorithm flow chart of AENNM.

Generally, the algorithm flow chart of AENNM is presented in Fig. 2 and the primary steps for employing the AENNM to solve the NLPDEs are as follows:

Step 1: The Riccati equation Eq. (2.5) is selected as the auxiliary equation, and its solution is employed as the activation function $\varphi(\cdot)$ in the NNs.

Step 2: The NNs model is constructed by selecting specific activation functions, the number of neurons, and the number of hidden layers, as shown in Fig. 1.

Step 3: A nonlinear algebraic equation governing the weights and biases is systematically derived via substitution of the trial function specified in Eq. (2.2) into the NLPDEs Eq. (2.1).

Step 4: By collecting coefficients of each term and equating them to zero, an under-determined system of nonlinear algebraic equations is obtained.

Step 5: The derived system of nonlinear algebraic equations is computationally solved employing Maple symbolic computation software.

Step 6: By substituting the obtained weights and biases along with the specific form Eq. (2.4) of $\varphi(\cdot)$ into NNs model Eq. (2.2), the analytical solution of Eq. (2.1) is derived.

3. Examples

In this section, several validation examples are considered to verify the effectiveness of auxiliary equation neural networks method for solving the NLPDEs.

Example 1. Consider the nonlinear evolution equation [40, 41] of the following form

$$u_{tt} + \alpha u_{xx} + \beta u + \gamma u^3 = 0, \quad (3.1)$$

where α , β , and γ are constants. Eq. (3.1) contains some particular important equations such as Duffing, Klein–Gordon, Landau–Ginsburg–Higgs, and ϕ^4 equations.

The 2-2-2-1 model is used to construct the potential analytical solution of Eq. (3.1), as shown in Fig. 1a. By setting $F_1(\xi_1) = \varphi(\xi_1)$, $F_2(\xi_2) = \varphi^2(\xi_2)$, $F_3(\xi_3) = (\xi_3)$, and $F_4(\xi_4) = (1/\xi_4)$ in Fig. 1a, and substituting them into Eq. (2.2), we obtain the following trial function

$$u(x, t) = w_{3u} \left(w_{13} \varphi(tw_{t1} + xw_{x1} + b_1) + w_{23} \varphi^2(tw_{t2} + xw_{x2} + b_2) + b_3 \right) + \frac{w_{4u}}{w_{14} \varphi(tw_{t1} + xw_{x1} + b_1) + w_{24} \varphi^2(tw_{t2} + xw_{x2} + b_2) + b_4} + b_5. \quad (3.2)$$

By substituting Eq. (3.2) into Eq. (3.1), the solution can be derived using AENNM as follows,

$$\left\{ \begin{array}{l} \alpha = -\frac{32b^3w_{24}^2w_{t2}^2 + \gamma w_{4u}^2}{32b^3w_{24}^2w_{x2}^2}, \beta = -\frac{\gamma w_{4u}^2}{8b^2w_{24}^2}, b = b, b_3 = b_3, b_4 = -bw_{24}, b_5 = \frac{w_{4u}}{2bw_{24}}, \\ w_{13} = 0, w_{14} = 0, w_{23} = w_{23}, w_{24} = w_{24}, w_{3u} = 0, w_{4u} = w_{4u}, w_{t1} = w_{t1}, \\ w_{t2} = w_{t2}, w_{x1} = w_{x1}, w_{x2} = w_{x2}. \end{array} \right\} \quad (3.3)$$

Substituting Eq. (3.3) into Eq. (3.2) yields the following analytical solution to the original equation,

$$u(x, t) = \frac{w_{4u}}{w_{24} \varphi^2(tw_{t2} + xw_{x2} + b_2) - bw_{24}} + \frac{w_{4u}}{2bw_{24}}. \quad (3.4)$$

When $b < 0$,

$$u(x, t) = \mp \frac{w_{4,u}}{2bw_{24} \cosh(2\sqrt{-b} (tw_{t2} + xw_{x2} + b_2))}. \quad (3.5)$$

If one chooses coefficients $\{b = -1, w_{x2} = 2, w_{t2} = 1, w_{24} = 2, w_{4u} = 1, b_2 = 1\}$ and take the "−" in the Eq. (3.5), we obtain Fig. 3. Then the behavior of the solution can be intuitively expressed. Fig. 3a is a three-dimensional diagram drawn based on the spatio-temporal domain $[-30, 30] \times [-30, 30]$. To observe the local behavior of the solution, we plot the x -curves in Fig. 3b at interval $t \in [-30, 30]$. And the contour and density plots of the solution are shown in Fig. 3c and Fig. 3d, respectively.

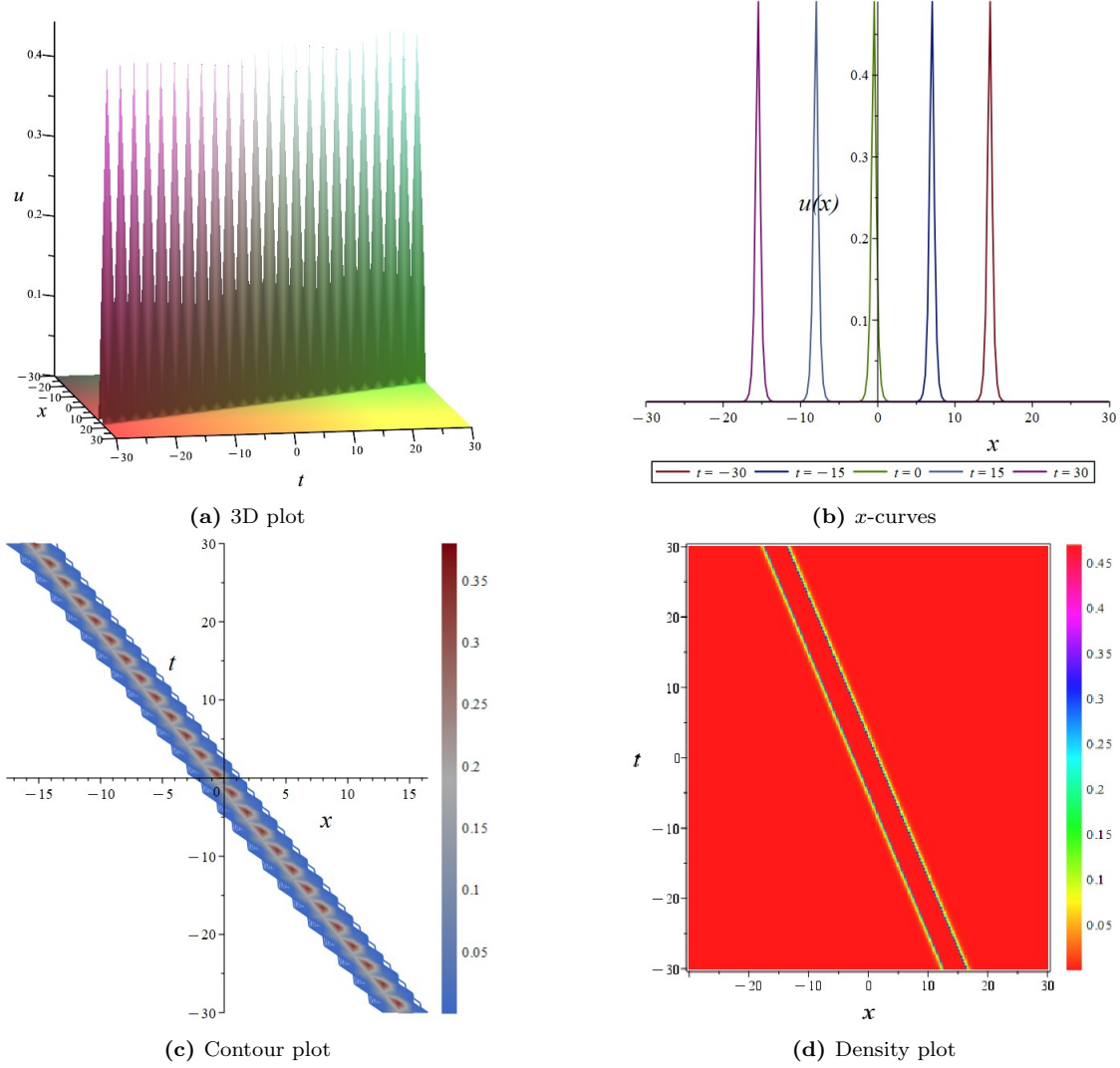


Fig. 3. The three-dimensional plot, curves plot, contour plot, and density plot of the solution Eq. (3.5).

When $b > 0$,

$$u(x, t) = \mp \frac{w_{4u}}{2bw_{24} \cos\left(2\sqrt{b}(tw_{t2} + xw_{x2} + b_2)\right)}. \quad (3.6)$$

Similarly, to better observe the properties of the solution, we take the coefficients $\{b = 3, w_{x2} = 2, w_{t2} = 1, w_{24} = 1, w_{4u} = 1, b_2 = 1\}$ and take the "−" in the Eq. (3.6).

The three-dimensional plot, contour plot, and density plot of the solution are displayed in Fig. 4 based on the spatio-temporal domain $[-30, 30] \times [-30, 30]$.

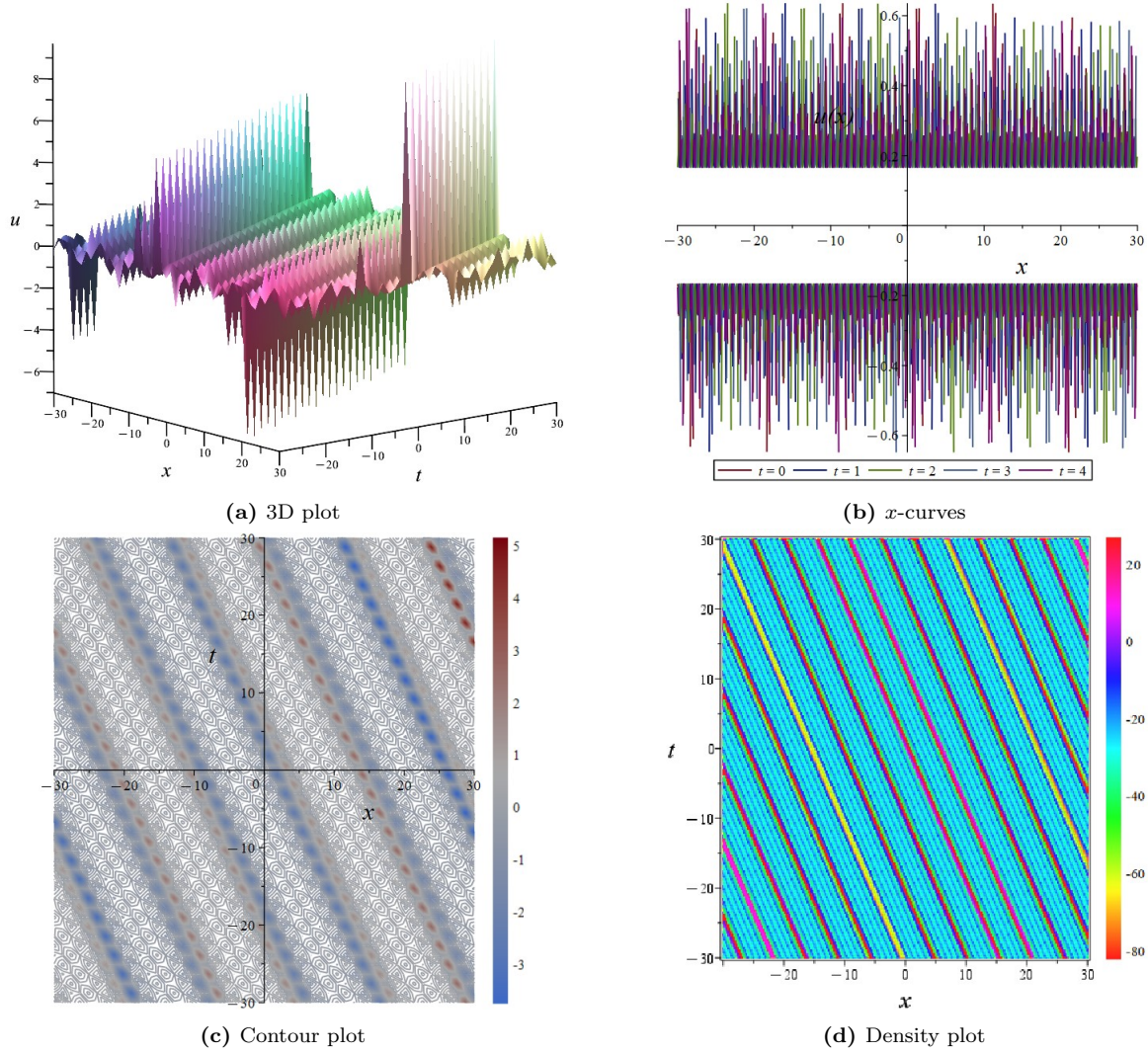


Fig. 4. The three-dimensional plot, curves plot, contour plot, and density plot of the solution Eq. (3.6).

Example 2. Consider the Korteweg-de Vries-Burgers equation [42] in the form

$$u_t + puu_x + qu^2u_x + ru_{xx} - su_{xxx} = 0, \quad (3.7)$$

where p , q , r , and s are constants. Eq. (3.7) can be regarded as a generalization of the Korteweg-de Vries (KdV), modified Korteweg-de Vries (mKdV), and Burgers equations, encompassing both nonlinear dispersion and dissipation effects.

The 2-2-2-1 model is used to construct the potential analytical solution of Eq. (3.7), as shown in Fig. 1a. By setting $F_1(\xi_1) = \varphi(\xi_1)$, $F_2(\xi_2) = \varphi(\xi_2)$, $F_3(\xi_3) = (\xi_3)$, $F_4(\xi_4) = (1/\xi_4)$

in Fig. 1a, and substituting them into Eq. (2.2), we obtain the following trial function

$$u(x, t) = w_{3u} (w_{13} \varphi(tw_{t1} + xw_{x1} + b_1) + w_{23} \varphi(tw_{t2} + xw_{x2} + b_2) + b_3) + \frac{w_{4u}}{w_{14} \varphi(tw_{t1} + xw_{x1} + b_1) + w_{24} \varphi(tw_{t2} + xw_{x2} + b_2) + b_4} + b_5. \quad (3.8)$$

By substituting Eq. (3.8) into Eq. (3.7), the following coefficient solutions are obtained via AENNM,

Solution 1:

$$\left\{ \begin{array}{l} p = p, q = q, r = r, s = \frac{w_{23}^2 w_{3u}^2 q}{6w_{x2}^2}, b = b, b_3 = \frac{-w_{3u}(2qb_5 + p)w_{23} - 2rw_{x2}}{2qw_{23}w_{3u}^2}, b_4 = 0, \\ b_5 = b_5, w_{13} = 0, w_{14} = w_{14}, w_{23} = w_{23}, w_{24} = 0, w_{3u} = w_{3u}, w_{4u} = 0, \\ w_{t1} = w_{t1}, w_{x1} = w_{x1}, w_{x2} = w_{x2}, w_{t2} = \frac{w_{x2}(4bq^2w_{23}^4w_{3u}^4 + 3p^2w_{23}^2w_{3u}^2 - 12r^2w_{x2}^2)}{12w_{23}^2qw_{3u}^2}. \end{array} \right\} \quad (3.9)$$

By substituting Eq. (3.9) into Eq. (3.8), the analytical solution of the original equation is obtained as follows,

$$u(x, t) = w_{3u} w_{23} \varphi \left(\frac{tw_{x2}(4bq^2w_{23}^4w_{3u}^4 + 3p^2w_{23}^2w_{3u}^2 - 12r^2w_{x2}^2)}{12w_{23}^2qw_{3u}^2} + xw_{x2} + b_2 \right) - \frac{p}{2q} - \frac{rw_{x2}}{qw_{23}w_{3u}}. \quad (3.10)$$

When $b < 0$,

$$u(x, t) = -w_{3u} w_{23} \sqrt{-b} \tanh \left(\sqrt{-b} (tw_{t2} + xw_{x2} + b_2) \right) - \frac{p}{2q} - \frac{rw_{x2}}{qw_{23}w_{3u}}, \quad (3.11a)$$

$$u(x, t) = -w_{3u} w_{23} \sqrt{-b} \coth \left(\sqrt{-b} (tw_{t2} + xw_{x2} + b_2) \right) - \frac{p}{2q} - \frac{rw_{x2}}{qw_{23}w_{3u}}, \quad (3.11b)$$

where w_{t2} is defined in Eq. (3.9).

When $b > 0$,

$$u(x, t) = w_{3u} w_{23} \sqrt{b} \tan \left(\sqrt{b} \xi_2 \right) - \frac{p}{2q} - \frac{rw_{x2}}{qw_{23}w_{3u}}, \quad (3.12a)$$

$$u(x, t) = -w_{3u} w_{23} \sqrt{b} \cot \left(\sqrt{b} (tw_{t2} + xw_{x2} + b_2) \right) - \frac{p}{2q} - \frac{rw_{x2}}{qw_{23}w_{3u}}, \quad (3.12b)$$

where w_{t2} is defined in Eq. (3.9).

When $b = 0$,

$$u(x, t) = -\frac{w_{3u} w_{23}}{tw_{t2} + xw_{x2} + b_2} - \frac{p}{2q} - \frac{rw_{x2}}{qw_{23}w_{3u}}, \quad (3.13)$$

where w_{t2} is defined in Eq. (3.9).

Solution 2:

$$\left\{ \begin{array}{l} p = -\frac{2w_{x1}(bw_{14}^2 + b_4^2)(6bsb_5w_{14}^2w_{x1} - rw_{14}w_{4u} + 6sb_4w_{x1}(b_4b_5 + w_{4u}))}{w_{4u}^2w_{14}^2}, q = \frac{6sw_{x1}^2(bw_{14}^2 + b_4^2)^2}{w_{4u}^2w_{14}^2}, \\ r = r, s = s, b = b, b_3 = b_3, b_4 = b_4, b_5 = b_5, w_{13} = w_{24} = w_{3u} = 0, \\ w_{14} = w_{14}, w_{23} = w_{23}, w_{4u} = w_{4u}, w_{x1} = w_{x1}, w_{x2} = w_{x2}, w_{t2} = w_{t2}, \\ w_{t1} = \frac{(6b^2sb_5^2w_{14}^4w_{x1} - 2brb_5w_{14}^3w_{4u} + (12b_4^2b_5^2 + 12b_4b_5w_{4u} + 2w_{4u}^2)sbw_{x1}w_{14}^2 - \Omega_1)w_{x1}^2}{w_{4u}^2w_{14}^2}, \\ \Omega_1 = 2rb_4w_{4u}(b_4b_5 + w_{4u})w_{14} + 6sb_4^2w_{x1}(b_4b_5 + w_{4u})^2. \end{array} \right\} \quad (3.14)$$

By substituting Eq. (3.14) into Eq. (3.8), the solution of the original equation is obtained as follows,

$$u(x, t) = \frac{w_{4u}}{w_{14} \varphi(tw_{t1} + xw_{x1} + b_1) + b_4} + b_5, \quad (3.15)$$

where w_{t1} is defined in Eq. (3.14).

When $b < 0$,

$$u(x, t) = \frac{w_{4u}}{-w_{14}\sqrt{-b} \tanh(\sqrt{-b} (tw_{t1} + xw_{x1} + b_1)) + b_4} + b_5, \quad (3.16a)$$

$$u(x, t) = \frac{w_{4u}}{-w_{14}\sqrt{-b} \coth(\sqrt{-b} (tw_{t1} + xw_{x1} + b_1)) + b_4} + b_5, \quad (3.16b)$$

where w_{t1} is defined in Eq. (3.14).

When $b > 0$,

$$u(x, t) = \frac{w_{4u}}{w_{14}\sqrt{b} \tan(\sqrt{b} \xi_1) + b_4} + b_5, \quad (3.17a)$$

$$u(x, t) = \frac{w_{4u}}{-w_{14}\sqrt{b} \cot(\sqrt{b} (tw_{t1} + xw_{x1} + b_1)) + b_4} + b_5, \quad (3.17b)$$

where w_{t1} is defined in Eq. (3.14).

When $b = 0$,

$$u(x, t) = \frac{w_{4u}}{-\frac{w_{14}}{tw_{t1} + xw_{x1} + b_1} + b_4} + b_5, \quad (3.18)$$

where w_{t1} is defined in Eq. (3.14).

Solution 3:

$$\left\{ \begin{array}{l} b = 0, p = p, q = q, r = -\frac{w_{23}w_{3u}(2qb_3w_{3u} + 2qb_5 + p)}{2w_{x2}}, s = \frac{w_{23}^2qw_{3u}^2}{6w_{x2}^2}, b_3 = b_3, b_4 = b_4, \\ b_5 = b_5, w_{13} = w_{14} = w_{4u} = 0, w_{23} = w_{23}, w_{24} = w_{24}, w_{3u} = w_{3u}, w_{t1} = w_{t1}, \\ w_{x1} = w_{x1}, w_{x2} = w_{x2}, w_{t2} = -(b_3w_{3u} + b_5)w_{x2}((b_3w_{3u} + b_5)q + p). \end{array} \right\} \quad (3.19)$$

By substituting Eq. (3.19) into Eq. (3.8) the solution of the Eq. (3.7) can ultimately be obtained as:

$$u(x, t) = \frac{w_{23}w_{3u}}{w_{x2}((b_3w_{3u} + b_5)(qb_3w_{3u} + qb_5 + p)t - x)} + b_3w_{3u} + b_5, \quad (3.20)$$

where w_{t2} is defined in Eq. (3.19).

Solution 4:

$$\left\{ \begin{array}{l} p = \frac{-2q(b_3w_{3u} + b_5)w_{4u} + 2brw_{24}w_{x2}}{w_{4u}}, \beta = \beta, q = q, s = \frac{qw_{4u}^2}{6b^2w_{24}^2w_{x2}^2}, b_3 = b_3, b_4 = 0, b_5 = b_5, \\ w_{13} = 0, w_{14} = 0, w_{23} = -\frac{w_{4u}}{bw_{24}w_{3u}}, w_{24} = w_{24}, w_{3u} = w_{3u}, w_{4u} = w_{4u}, w_{t1} = w_{t1}, \\ w_{x1} = w_{x1}, w_{x2} = w_{x2}, w_{t2} = -\frac{(6b^2rw_{x2}(b_3w_{3u} + b_5)w_{24}^3 - 3bqw_{4u}(b_3w_{3u} + b_5)^2w_{24}^2 - 4qw_{4u}^3)w_{x2}}{3bw_{24}^2w_{4u}}. \end{array} \right\} \quad (3.21)$$

The solution $u(x, t)$ corresponding to this set of constraints is as follows,

$$u(x, t) = -\frac{w_{4u}\varphi(tw_{t2} + xw_{x2} + b_2)}{bw_{24}} + \frac{w_{4u}}{w_{24}\varphi(tw_{t2} + xw_{x2} + b_2)} + b_3w_{3u} + b_5, \quad (3.22)$$

where w_{t2} is defined in Eq. (3.21).

When $b < 0$,

$$u(x, t) = \frac{-w_{4u}(\tanh(\sqrt{-b}(tw_{t2} + xw_{x2} + b_2)) + \coth(\sqrt{-b}(tw_{t2} + xw_{x2} + b_2)))}{\sqrt{-b}w_{24}} + b_3w_{3u} + b_5, \quad (3.23)$$

where w_{t2} is defined in Eq. (3.21).

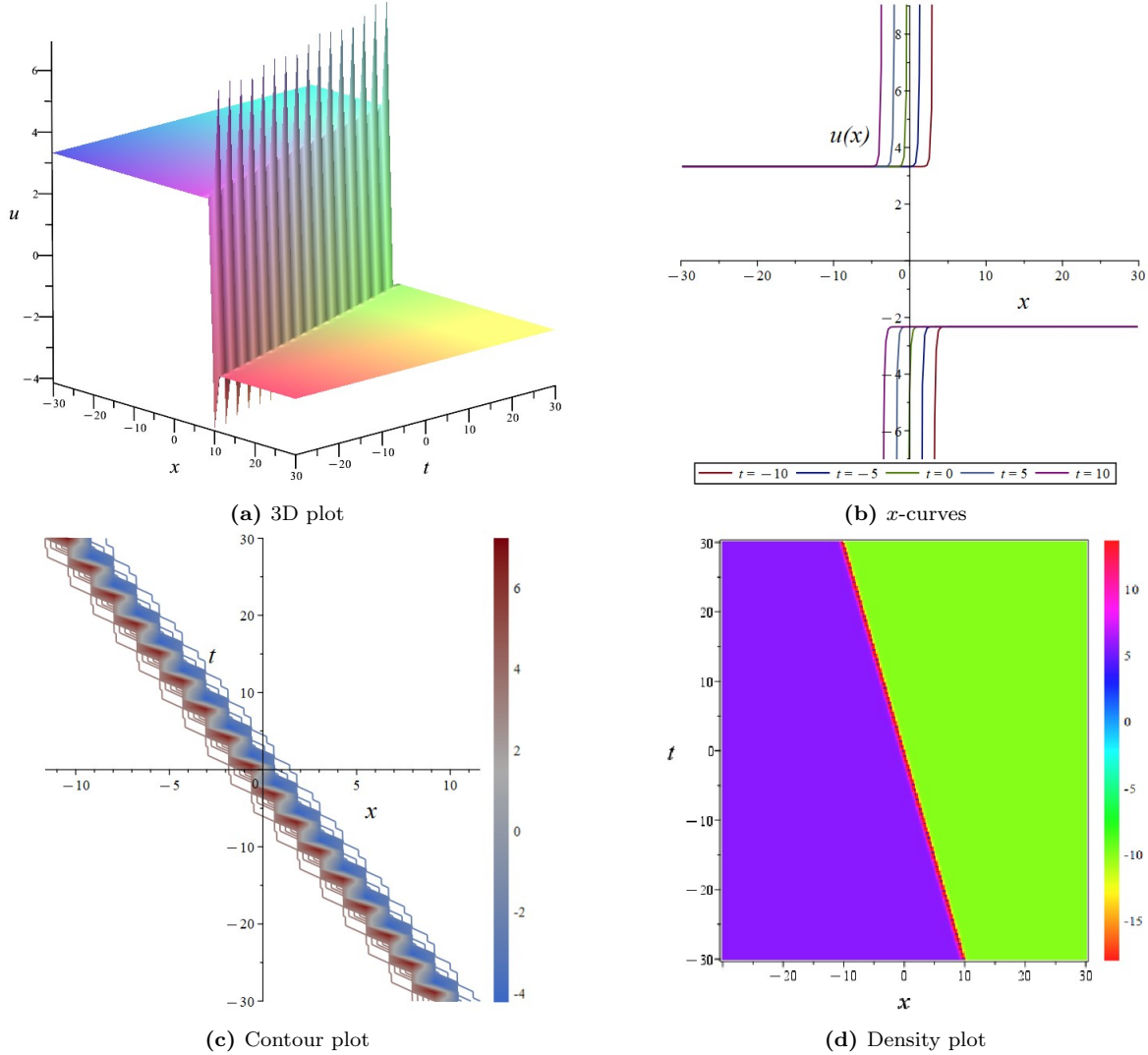


Fig. 5. The three-dimensional plot, curves plot, contour plot, and density plot of the solution Eq. (3.23).

If one chooses coefficients $\{b = -0.5, q = 1, r = 1, w_{x2} = 2, w_{24} = 1, w_{3u} = 1, w_{4u} = 1, b_2 = 0.5, b_3 = 0.5, b_5 = 0.5\}$ in the Eq. (3.23), we obtain Fig. 5. Then the behavior of

the solution can be intuitively expressed. Fig. 5a is a three-dimensional diagram drawn based on the spatio-temporal domain $[-30, 30] \times [-30, 30]$. To observe the local behavior of the solution, we plot the x -curves in Fig. 5b at interval $t \in [-30, 30]$. And the contour and density plots of the solution are shown in Fig. 5c and Fig. 5d, respectively.

When $b > 0$,

$$u(x, t) = \frac{w_{4u} \left(\cot \left(\sqrt{b} (tw_{t2} + xw_{x2} + b_2) \right) - \tan \left(\sqrt{b} (tw_{t2} + xw_{x2} + b_2) \right) \right)}{\sqrt{b} w_{24}} \quad (3.24)$$

$$+ b_3 w_{3u} + b_5,$$

where w_{t2} is defined in Eq. (3.21).

Similarly, to better observe the properties of the solution, we take the coefficients $\{b = 3, q = 1, r = 1, w_{x2} = 1, w_{24} = 1, w_{3u} = 1, w_{4u} = 1, b_2 = 2, b_3 = 1, b_5 = 1\}$ in the Eq. (3.24). The three-dimensional plot, contour plot, and density plot of the solution are displayed in Fig. 6 based on the spatio-temporal domain $[-10, 10] \times [-10, 10]$.

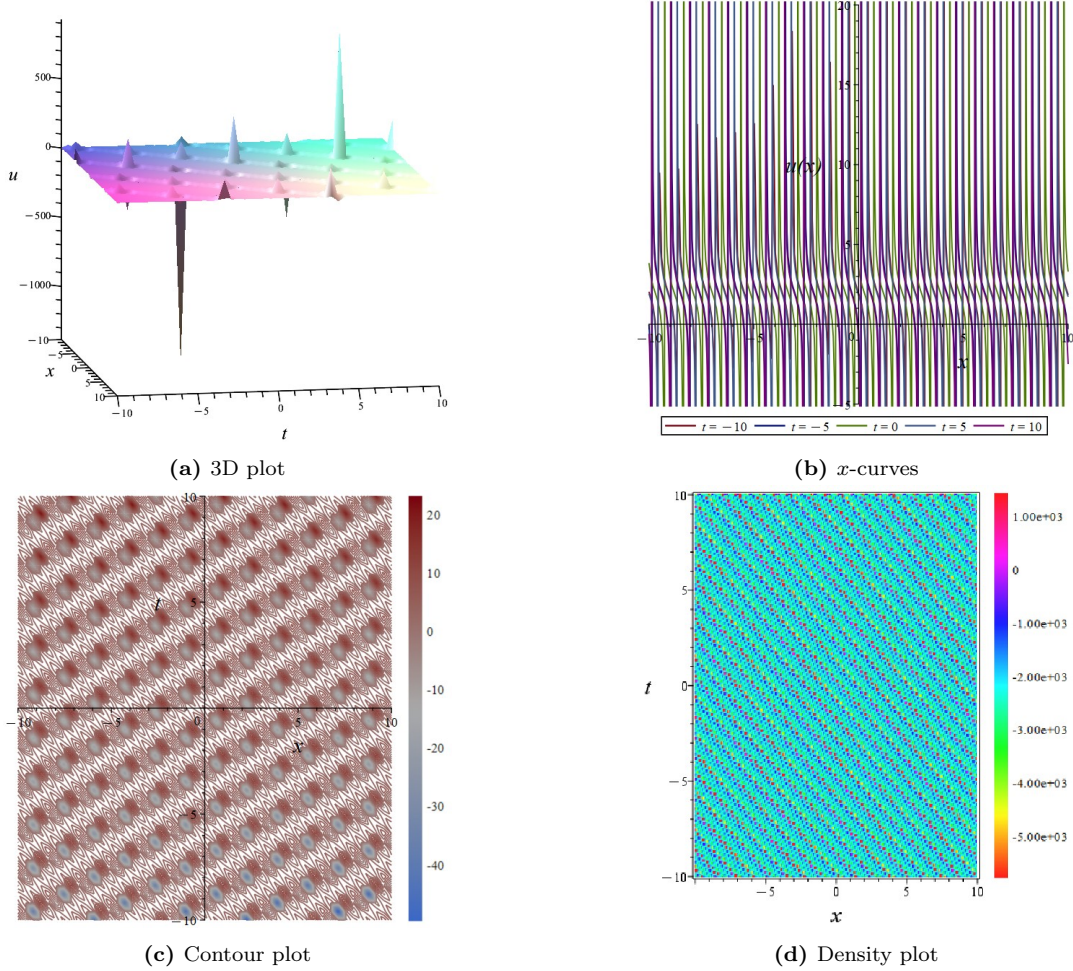


Fig. 6. The three-dimensional plot, curves plot, contour plot, and density plot of the solution Eq. (3.24).

Example 3. Consider the (2+1)-dimensional generalization of Boussinesq equation [42]

$$u_{tt} - u_{xx} - u_{yy} - (u^2)_{xx} - u_{xxxx} = 0. \quad (3.25)$$

The 3-2-2-1 model is used to construct the potential analytical solution of Eq. (3.1), as shown in Fig. 1b. By setting $F_1(\xi_1) = \varphi(\xi_1)$, $F_2(\xi_2) = \varphi(\xi_2)$, $F_3(\xi_3) = (\xi_3)^2$, and $F_4(\xi_4) = (1/\xi_4)^2$ in Fig. 1b, and substituting them into Eq. (2.2), we obtain the following trial function

$$\begin{aligned} u(x, y, t) = & w_{3u} (w_{13}\varphi(tw_{t1} + xw_{x1} + yw_{y1} + b_1) + w_{23}\varphi(tw_{t2} + xw_{x2} + yw_{y2} + b_2) + b_3)^2 \\ & + \frac{w_{4u}}{(w_{14}\varphi(tw_{t1} + xw_{x1} + yw_{y1} + b_1) + w_{24}\varphi(tw_{t2} + xw_{x2} + yw_{y2} + b_2) + b_4)^2} \\ & + b_5. \end{aligned} \quad (3.26)$$

By substituting Eq. (3.26) into Eq. (3.25), the following coefficient solutions are obtained via AENNM,

Solution 1:

$$\left\{ \begin{array}{l} b = b, b_3 = b_3, b_4 = 0, b_5 = \frac{-8bw_{x2}^4 + w_{t2}^2 - w_{x2}^2 - w_{y2}^2}{2w_{x2}^2}, w_{13} = w_{14} = w_{4u} = 0, \\ w_{23} = w_{23}, w_{24} = w_{24}, w_{3u} = -\frac{6w_{x2}^2}{w_{23}^2}, w_{t1} = w_{t1}, w_{t2} = w_{t2}, w_{x1} = w_{x1}, \\ w_{x2} = w_{x2}, w_{y1} = w_{y1}, w_{y2} = w_{y2}. \end{array} \right\} \quad (3.27)$$

By substituting Eq. (3.27) into Eq. (3.26), the analytical solution of the original equation is obtained as follows,

$$u(x, t) = -6w_{x2}^2 \varphi^2(tw_{t2} + xw_{x2} + yw_{y2} + b_2) - \frac{8bw_{x2}^4 - w_{t2}^2 + w_{x2}^2 + w_{y2}^2}{2w_{x2}^2}. \quad (3.28)$$

When $b < 0$,

$$u(x, t) = 6w_{x2}^2 b \tanh^2 \left(\sqrt{-b} \xi_2 \right) - \frac{8bw_{x2}^4 - w_{t2}^2 + w_{x2}^2 + w_{y2}^2}{2w_{x2}^2}, \quad (3.29a)$$

$$u(x, t) = 6w_{x2}^2 b \coth^2 \left(\sqrt{-b} \xi_2 \right) - \frac{8bw_{x2}^4 - w_{t2}^2 + w_{x2}^2 + w_{y2}^2}{2w_{x2}^2}, \quad (3.29b)$$

where $\xi_2 = tw_{t2} + yw_{y2} + xw_{x2} + b_2$.

When $b > 0$,

$$u(x, t) = -6w_{x2}^2 b \tan^2 \left(\sqrt{b} \xi_2 \right) - \frac{8bw_{x2}^4 - w_{t2}^2 + w_{x2}^2 + w_{y2}^2}{2w_{x2}^2}, \quad (3.30a)$$

$$u(x, t) = -6w_{x2}^2 b \cot^2 \left(\sqrt{b} \xi_2 \right) - \frac{8bw_{x2}^4 - w_{t2}^2 + w_{x2}^2 + w_{y2}^2}{2w_{x2}^2}, \quad (3.30b)$$

where $\xi_2 = tw_{t2} + yw_{y2} + xw_{x2} + b_2$.

When $b = 0$,

$$u(x, t) = -\frac{6w_{x2}^2}{(tw_{t2} + xw_{x2} + yw_{y2} + b_2)^2} + \frac{w_{t2}^2 - w_{x2}^2 - w_{y2}^2}{2w_{x2}^2}. \quad (3.31)$$

Solution 2:

$$\left\{ \begin{array}{l} b = b, b_3 = 0, b_4 = 0, b_5 = \frac{-8bw_{x2}^4 + w_{t2}^2 - w_{x2}^2 - w_{y2}^2}{2w_{x2}^2}, w_{13} = w_{14} = 0, w_{23} = w_{23}, \\ w_{24} = w_{24}, w_{3u} = -\frac{6w_{x2}^2}{w_{23}^2}, w_{4,u} = -6w_{x2}^2 b^2 w_{24}^2, w_{t1} = w_{t1}, w_{t2} = w_{t2}, \\ w_{x1} = w_{x1}, w_{x2} = w_{x2}, w_{y1} = w_{y1}, w_{y2} = w_{y2}. \end{array} \right\} \quad (3.32)$$

By substituting Eq. (3.32) into Eq. (3.26), the solution of the Eq. (3.25) can ultimately be obtained as

$$u(x, t) = -6w_{x2}^2 \varphi^2(tw_{t2} + xw_{x2} + yw_{y2} + b_2) - \frac{6w_{x2}^2 b^2}{\varphi^2(tw_{t2} + xw_{x2} + yw_{y2} + b_2)} - \frac{8bw_{x2}^4 - w_{t2}^2 + w_{x2}^2 + w_{y2}^2}{2w_{x2}^2}. \quad (3.33)$$

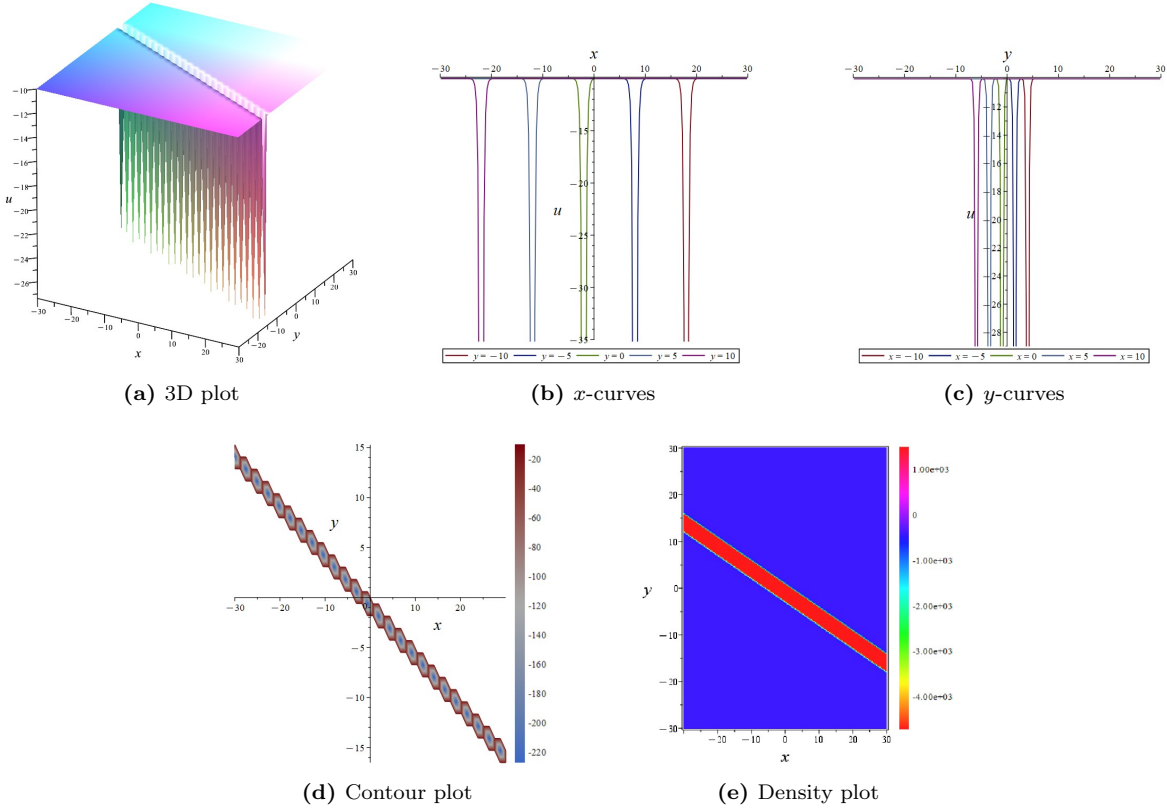


Fig. 7. The three-dimensional plot, curves plot, contour plot, and density plot of the solution Eq. (3.34a).

When $b < 0$,

$$u(x, t) = 6w_{x2}^2 b \tanh^2(\sqrt{-b} \xi_2) + \frac{6w_{x2}^2 b}{\tanh^2(\sqrt{-b} \xi_2)} - \frac{8bw_{x2}^4 - w_{t2}^2 + w_{x2}^2 + w_{y2}^2}{2w_{x2}^2}, \quad (3.34a)$$

$$u(x, t) = 6w_{x2}^2 b \coth^2(\sqrt{-b} \xi_2) + \frac{6w_{x2}^2 b}{\coth^2(\sqrt{-b} \xi_2)} - \frac{8bw_{x2}^4 - w_{t2}^2 + w_{x2}^2 + w_{y2}^2}{2w_{x2}^2}, \quad (3.34b)$$

where $\xi_2 = tw_{t2} + yw_{y2} + xw_{x2} + b_2$.

If one chooses coefficients $\{b = -1, w_{x2} = 1, w_{y2} = 2, w_{t2} = 1, b_2 = 1\}$ and take $t = 1$ in the Eq. (3.34a), we obtain Fig. 7. Then the behavior of the solution can be intuitively expressed. Fig. 7a is a three-dimensional diagram drawn based on the spatio-temporal domain $[-30, 30] \times [-30, 30]$. To observe the local behavior of the solution, we plot the x -curves in Fig. 7b at interval $t \in [-30, 30]$. And the contour and density plots of the solution are shown in Fig. 7c and Fig. 7d, respectively.

When $b > 0$,

$$u(x, t) = -6w_{x2}^2 b \tan^2(\sqrt{b} \xi_2) - \frac{6w_{x2}^2 b}{\tan^2(\sqrt{b} \xi_2)} - \frac{8bw_{x2}^4 - w_{t2}^2 + w_{x2}^2 + w_{y2}^2}{2w_{x2}^2}, \quad (3.35a)$$

$$u(x, t) = -6w_{x2}^2 b \cot^2(\sqrt{b} \xi_2) - \frac{6w_{x2}^2 b}{\cot^2(\sqrt{b} \xi_2)} - \frac{8bw_{x2}^4 - w_{t2}^2 + w_{x2}^2 + w_{y2}^2}{2w_{x2}^2}, \quad (3.35b)$$

where $\xi_2 = tw_{t2} + yw_{y2} + xw_{x2} + b_2$.

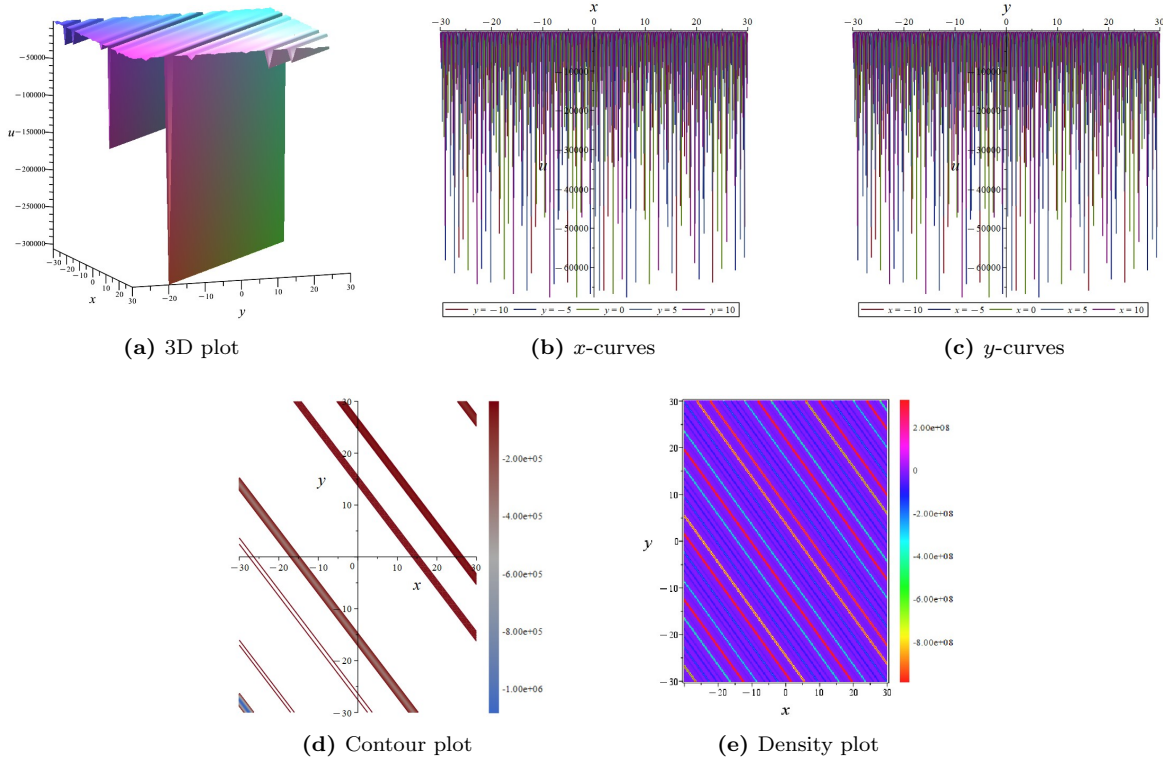


Fig. 8. The three-dimensional plot, curves plot, contour plot, and density plot of the solution Eq. (3.35a).

Similarly, to better observe the properties of the solution, we take the coefficients $\{b = 1, w_{x2} = 2, w_{y2} = 2, w_{t2} = 1, b_2 = 1\}$ and let $t = 1$ in the Eq. (3.35a). The three-dimensional plot, contour plot, and density plot of the solution are displayed in Fig. 8 based on the spatio-temporal domain $[-30, 30] \times [-30, 30]$.

4. Comparison

In this section, nonlinear evolution Eq. (3.1) are studied to demonstrate that the proposed method can not only obtain solutions already available in the literature but also yield novel and interesting results.

To further confirm the flexibility and customizability of our method, we employ different neural networks architectures to solve the Eq. (3.1). The 2-2-2-1 model is used to construct the potential analytical solution of equation, as shown in Fig. 1a. Letting $F_1(\xi_1) = \varphi(\xi_1)$, $F_2(\xi_2) = \varphi(\xi_2)$, $F_3(\xi_3) = (\xi_3)$, and $F_4(\xi_4) = (1/\xi_4)$ in Fig. 1a. And by substituting Eq. (3.8) into Eq. (3.1), the following coefficient solutions are obtained via AENNM,

Solution 1:

$$\left\{ \begin{array}{l} b = b, \alpha = \frac{-\gamma w_{13}^2 w_{3u}^2 - 2w_{t1}^2}{2w_{x1}^2}, \beta = \gamma b w_{13}^2 w_{3u}^2, b_3 = -\frac{b_5}{w_{3u}}, b_4 = 0, b_5 = b_5, \\ w_{13} = w_{13}, w_{14} = w_{14}, w_{23} = w_{24} = w_{4u} = 0, w_{3u} = w_{3u}, w_{t1} = w_{t1}, \\ w_{t2} = w_{t2}, w_{x1} = w_{x1}, w_{x2} = w_{x2}. \end{array} \right\} \quad (4.1)$$

By substituting Eq. (4.1) into Eq. (3.8), the analytical solution of the original equation is obtained as follows,

$$u(x, t) = w_{13} w_{3u} \varphi(t w_{t1} + x w_{x1} + b_1). \quad (4.2)$$

When $b < 0$,

$$u(x, t) = -w_{3u} w_{13} \sqrt{-b} \tanh\left(\sqrt{-b} (t w_{t1} + x w_{x1} + b_1)\right). \quad (4.3a)$$

$$u(x, t) = -w_{3u} w_{13} \sqrt{-b} \coth\left(\sqrt{-b} (t w_{t1} + x w_{x1} + b_1)\right). \quad (4.3b)$$

When $b > 0$,

$$u(x, t) = w_{3u} w_{13} \sqrt{b} \tan\left(\sqrt{b} (t w_{t1} + x w_{x1} + b_1)\right). \quad (4.4a)$$

$$u(x, t) = -w_{3u} w_{13} \sqrt{b} \cot\left(\sqrt{b} (t w_{t1} + x w_{x1} + b_1)\right). \quad (4.4b)$$

If take the coefficients $\{b = -\beta/2(\alpha + \lambda^2), w_{t1} = \lambda, b_1 = 0, w_{3u} w_{13} = \pm \sqrt{-2(\alpha + \lambda^2)/\gamma}, w_{x1} = 1\}$ in the Eq. (4.3a) and Eq. (4.4a), $\{b = -\beta/2(\alpha + \lambda^2), w_{t1} = \lambda, w_{x1} = 1, w_{3u} w_{13} = \mp \sqrt{-2(\alpha + \lambda^2)/\gamma}, b_1 = 0\}$ in the Eq. (4.3b) and Eq. (4.4b), the solutions obtained above are exactly the same as the true analytical solutions of [41] for Eq. (3.1).

Solution 2:

$$\left\{ \begin{array}{l} b = b, \alpha = -\frac{\gamma w_{23}^2 w_{3u}^2 + 2w_{t2}^2}{2w_{x2}^2}, \beta = -2\gamma b w_{23}^2 w_{3u}^2, b_3 = -\frac{b_5}{w_{3u}}, b_4 = 0, b_5 = b_5, \\ w_{13} = w_{14} = 0, w_{23} = w_{23}, w_{24} = w_{24}, w_{3u} = w_{3u}, w_{4u} = b w_{23} w_{24} w_{3u}, \\ w_{t1} = w_{t1}, w_{t2} = w_{t2}, w_{x1} = w_{x1}, w_{x2} = w_{x2}. \end{array} \right\} \quad (4.5)$$

By substituting Eq. (4.5) into Eq. (3.8), the solution of the original Eq. (3.1) can be obtained as

$$u(x, t) = w_{23}w_{3u} \varphi(tw_{t2} + xw_{x2} + b_2) + \frac{bw_{23}w_{3u}}{\varphi(tw_{t2} + xw_{x2} + b_2)}. \quad (4.6)$$

When $b < 0$,

$$u(x, t) = \pm w_{23}w_{3u} \sqrt{-b} \operatorname{csch}\left(\sqrt{-b} (tw_{t2} + xw_{x2} + b_2)\right) \operatorname{sech}\left(\sqrt{-b} (tw_{t2} + xw_{x2} + b_2)\right). \quad (4.7)$$

When $b > 0$,

$$u(x, t) = \pm w_{23}w_{3u} \sqrt{b} \sec\left(\sqrt{b} (tw_{t2} + xw_{x2} + b_2)\right) \csc\left(\sqrt{b} (tw_{t2} + xw_{x2} + b_2)\right). \quad (4.8)$$

If take the coefficients $\{b = \beta/4(\alpha + \lambda^2), w_{t2} = \lambda, w_{x2} = 1, w_{23}w_{3u} = \sqrt{-2(\alpha + \lambda^2)}/\gamma, b_2 = 0\}$ in the Eq. (4.7), $\{b = \beta/\alpha + \lambda^2, w_{t1} = \lambda, w_{x1} = 1, w_{23}w_{3u} = \sqrt{-2(\alpha + \lambda^2)}/\gamma, b_2 = 0\}$ in the Eq. (4.8), the solutions obtained above are exactly the same as the true analytical solutions of [41] for Eq. (3.1).

Solution 3:

$$\left\{ \begin{array}{l} b = b, \alpha = -\frac{\gamma w_{23}^2 w_{3u}^2 + 2w_{t2}^2}{2w_{x2}^2}, \beta = 4\gamma b w_{23}^2 w_{3u}^2, b_3 = -\frac{b_5}{w_{3u}}, b_4 = 0, b_5 = b_5, \\ w_{13} = w_{14} = 0, w_{23} = w_{23}, w_{24} = w_{24}, w_{3u} = w_{3u}, w_{4u} = -b w_{23} w_{24} w_{3u}, \\ w_{t1} = w_{t1}, w_{t2} = w_{t2}, w_{x1} = w_{x1}, w_{x2} = w_{x2}. \end{array} \right\} \quad (4.9)$$

By substituting Eq. (4.9) into Eq. (3.8), the analytical solution of the original equation is obtained as follows,

$$u(x, t) = w_{23}w_{3u} \varphi(tw_{t2} + xw_{x2} + b_2) - \frac{bw_{23}w_{3u}}{\varphi(tw_{t2} + xw_{x2} + b_2)}. \quad (4.10)$$

When $b < 0$,

$$u(x, t) = -w_{23}w_{3u} \sqrt{-b} \left(\tanh\left(\sqrt{-b} \xi_2\right) + \coth\left(\sqrt{-b} \xi_2\right) \right), \quad (4.11)$$

where $\xi_2 = tw_{t2} + xw_{x2} + b_2$.

When $b > 0$,

$$u(x, t) = w_{23}w_{3u} \sqrt{b} \left(\tan\left(\sqrt{b} \xi_2\right) - \cot\left(\sqrt{b} \xi_2\right) \right), \quad (4.12)$$

where $\xi_2 = tw_{t2} + xw_{x2} + b_2$.

If take the coefficients $\{b = -\beta/8(\alpha + \lambda^2), w_{t2} = \lambda, b_2 = 0, w_{23}w_{3u} = \mp \sqrt{-2(\alpha + \lambda^2)}/\gamma, w_{x2} = 1\}$ in the Eq. (4.11) and Eq. (4.12), the solutions obtained above are exactly the same as the true analytical solutions of [41] for Eq. (3.1).

Therefore, the solution obtained by the proposed method can yield the solutions derived using the modified extended tanh-function method [41] by taking specific values for the coefficients. Moreover, the solutions obtained by AENNM not only include those

derived from existing methods in the literature but can also yield new solutions, such as Eq. (3.5) and Eq. (3.6).

Remark 1. This paper presents a variety of NNs architectures designed for obtaining analytical solutions to NLPDEs. Owing to the method’s significant flexibility and adaptability, different networks configurations can be employed to derive novel types of solutions for these equations.

Remark 2. To verify the reliability of the results, the derived analytical solutions are substituted back into the original equations, confirming that both sides remain equivalent. All solutions obtained by the analytical method presented in this study have been rigorously validated using Maple software.

5. Discussions

This paper proposes a novel method that combines NNs models with symbolic computation techniques to rapidly obtain exact analytical solutions for NLPDEs. Compared to traditional NNs approaches [31–34], this method solely utilizes the feedforward computation of NNs to construct trial functions for the equations, without incorporating the training mechanism of NNs. Therefore, the proposed approach eliminates the need for iterative calculations and optimization procedures. Furthermore, this approach yields exact solutions to the equations without data samples, ensuring zero approximation error. This paper introduces a novel approach to obtain exact solutions of NLPDEs which has the potential to advance the field by providing solutions without the need for large datasets or iterative optimization.

Traditional symbolic computation methods, such as the extended tanh-function method, are applicable to NLPDEs that can be transformed into ordinary differential equations via traveling wave transformations. When using such methods, the form of the preset solution is fixed. Moreover, traditional symbolic computation approaches require tailored solution strategies for different equations. In contrast, the proposed method in this paper does not rely on traveling wave transformations but instead directly employs a NNs structure to construct trial functions for the given equations. By leveraging the NNs architecture, the design of trial functions becomes more systematic and explicit.

Recently, the bilinear neural network method (BNNM) [35] has been successfully applied to solve various NLPDEs, including the Caudrey-Dodd-Gibbon-Kotera-Sawada-like equation [43], the Boussinesq equation [44], the extended Sawada-Kotera equation [45], and the Boiti–Leon–Manna–Pempinelli-like equation [46]. However, BNNM requires complex preprocessing of the equations, namely bilinear transformation, which poses a challenge for researchers without a strong mathematical background. Moreover, not all partial differential equations possess a bilinear form, further limiting the applicability of this method. Unlike BNNM, the method proposed in this paper does not require bilinear transformation of the equations, thereby lowering the barrier for researchers.

However, the proposed method also has certain limitations as follows: (i) Designing appropriate neural networks architectures is crucial for solving NLPDEs. Only by establishing suitable networks structures can optimal solutions be obtained. (ii) As the complexity of neural networks models increases, the computational workload grows correspondingly.

6. Conclusions

In this study, we propose the auxiliary equation neural networks method (AENNM) to analytically solve NLPDEs. This method introduces a novel activation function derived from solutions of the Riccati equation for NNs, establishing a new connection between differential equations and deep learning. The method introduces a novel interpretable activation function for NNs, enabling the systematic construction of new trial functions for NLPDEs within the "2-2-2-1" and "3-2-2-1" networks architectures. The feasibility of this method is demonstrated by solving the nonlinear evolution equation, the Korteweg-de Vries-Burgers equation, and the (2+1)-dimensional Boussinesq equation. Due to embedding the auxiliary equation method into the NNs framework, some new and interesting solutions are obtained. The solutions expressed in terms of hyperbolic, trigonometric, and rational functions provide valuable insights into the dynamic behaviors of the systems described by these equations. Three-dimensional plots, contour plots, and density plots are given to observe the dynamic behaviors of the obtained solutions.

Compared to traditional neural network methods, AENNM effectively balances the strong expressive power of neural networks with the high precision of symbolic computation. As a result, the proposed method achieves enhanced computational efficiency while maintaining high accuracy. Furthermore, the flexibility and adaptability of AENNM allow it to be applied to a wide range of NLPDEs by adjusting the network architecture, including the number of layers, neurons, and activation functions. The proposed method does not rely on traveling wave transformations, but instead embeds the solution of the equation as an activation function within the neural network architecture. Compared to existing methods in the literature, AENNM not only recovers known solutions but also discovers previously unreported ones, thereby enhancing our understanding of NLPDEs. The successful application of AENNM highlights its potential as a powerful tool for tackling complex nonlinear problems across diverse fields such as physics, engineering, and applied mathematics. Future research may focus on further refining the method, exploring its applicability to more intricate equations, and potentially integrating it with other advanced techniques to expand its capabilities.

Acknowledgements

This work was supported by the Natural Science Foundation of Shandong Province under Grant No.ZR2023MA062, the Belt and Road Special Foundation of The National Key Laboratory of Water Disaster Prevention under Grant No.2023491911, Tianyuan Fund for Mathematics of the National Natural Science Foundation of China under Grant No.12426105, and the Scientific and Technological Innovation Programs (STIP) of Higher Education Institutions in Shanxi under Grant No.2024L022.

Data availability

No data was used for the research described in the article.

Conflict of interest

The authors declare that they have no conflicts of interest.

References

- [1] X. Sang, H.H. Dong, Y. Fang, et al., Soliton, breather and rogue wave solutions of the nonlinear Schrödinger equation via Darboux transformation on a time–space scale, *Chaos, Solitons & Fractals*. **184** (2024) 115052.
- [2] N. Chen, F.S. Li, P.H. Wang, Global existence and blow-up phenomenon for a nonlocal semilinear pseudo-parabolic p-Laplacian equation, *Journal of Differential Equations*. **409** (2024) 395-440.
- [3] S.M. Wang, A. Batool, X. Sun, et al., Non-intrusive reduced-order model for time-dependent stochastic partial differential equations utilizing dynamic mode decomposition and polynomial chaos expansion, *Chaos*. **34** (7) (2024) 073102.
- [4] M.M. Roshid, M.M. Rahman, Bifurcation analysis, modulation instability and optical soliton solutions and their wave propagation insights to the variable coefficient nonlinear Schrödinger equation with Kerr law nonlinearity, *Nonlinear Dynamics*. **112** (18) (2024) 16355-16377.
- [5] M.Z. Yousaf, M. Abbas, M.K. Iqbal, et al., Abundant different types of soliton solutions with stability analysis for the $(2 + 1)$ -dimensional extended shallow water wave equation in ocean engineering with applications, *Nonlinear Dynamics*. **113** (4) (2025) 3713-3733.
- [6] J. Zhang, J. Manafian, S. Raut, S. Roy, et al., Study of two soliton and shock wave structures by weighted residual method and Hirota bilinear approach, *Nonlinear Dynamics*. **112** (14) (2024) 12375-12391.
- [7] L. Yang, B. Gao, The nondegenerate solitons solutions for the generalized coupled higher-order nonlinear Schrödinger equations with variable coefficients via the Hirota bilinear method, *Chaos, Solitons & Fractals*. **184** (2024) 115009.
- [8] H.L. Wu, Q.Y. Chen, J.F. Song, Backlund transformation, residual symmetry and exact interaction solutions of an extended $(2+1)$ -dimensional Korteweg-de Vries equation, *Applied Mathematics Letters*. **124** (2022) 107640.
- [9] Y. Liu, J.C. Wei, W. Yang, Lump type solutions: Bäcklund transformation and spectral properties, *Physica D: Nonlinear Phenomena*. **470** (2024) 134394.
- [10] U.K. Manda, S. Malik, S. Kumar, Y. Zhang, et al., Integrability aspects, rational type solutions and invariant solutions of an extended $(3 + 1)$ -dimensional B-type Kadomtsev–Petviashvili equation, *Chaos, Solitons & Fractals*. **181** (2024) 114689.
- [11] H. Sasaki, On inverse scattering for the two-dimensional nonlinear Schrödinger equation, *Journal of Differential Equations*. **401** (2024) 308-333.
- [12] M.R. Ali, M.A. Khattab, S.M. Mabrouk, Travelling wave solution for the Landau-Ginzburg-Higgs model via the inverse scattering transformation method, *Nonlinear Dynamics*. **111** (8) (2023) 7687-7697.

- [13] Y. Zhang, Y. Ren, H.H. Dong, Soliton solution to the complex modified Korteweg–de Vries equation on both zero and nonzero background via the robust inverse scattering method, *Communications in Theoretical Physics*. **74** (7) (2022) 34-44.
- [14] I.K. Muhammad, K. Abdullah, F. Aamir, Analyzing the Kuralay-II equation: bifurcation, chaos, and sensitivity insights through conformable derivative and Jacobi elliptic function expansion, *Physica Scripta*. **99** (9) (2024) 095210.
- [15] A. Farooq, K. Aamir, I. Muhammad, W.X. Ma, Exact solutions for the improved mKdv equation with conformable derivative by using the Jacobi elliptic function expansion method, *Optical and Quantum Electronics*. **56** (4) (2024) 542.
- [16] Y. Tian, Quasi hyperbolic function expansion method and tanh-function method for solving vibrating string equation and elastic rod equation, *Journal of Low Frequency Noise Vibration and Active Control*. **38** (3) (2019) 1455-1465.
- [17] M.B. Almatrafi, Solitary wave solutions to a fractional model using the improved modified extended tanh-function method, *Fractal & Fractional*. **7** (3) (2023) 252.
- [18] S.A. El-Tantawy, A.H. Salas, M.R. Alharthi, Novel analytical cnoidal and solitary wave solutions of the Extended Kawahara equation, *Fractal & Fractional*. **147** (2021) 110965.
- [19] B. Kaur, R.K. Gupta, Dispersion analysis and improved F-expansion method for space–time fractional differential equations, *Nonlinear Dynamics*. **96** (2) (2019) 837-852.
- [20] J. Muhammad, N. Nasreen, E. Hussain, U. Younas, et al., On the study of analytical soliton solutions and interaction aspects to the Estevez-Mansfield-Clarkson equation arising in diversity of fields, *Physica Scripta*. **99** (11) (2024) 115221.
- [21] R.A. Mohamed, A.K. Mahmoud, S.M. Mabrouk, Investigation of travelling wave solutions for the (3+1)-dimensional hyperbolic nonlinear Schrödinger equation using Riccati equation and F-expansion techniques, *Optical and Quantum Electronics*. **55** (11) (2023) 1-16.
- [22] K.K. Ali, D.Y. Sucu, S.B.G. Karakoc, Two effective methods for solution of the Gardner–Kawahara equation arising in wave propagation, *Mathematics and Computers in Simulation*. **220** (2024) 192-203.
- [23] A. Burcu, B. Ahmet, The (G'/G) -expansion method for the nonlinear lattice equations, *Communications in Nonlinear Science and Numerical Simulation*. **17** (9) (2012) 3490-3498.
- [24] M.L. Wang, X.Z. Li, J.L. Zhang, The (G'/G) -expansion method and travelling wave solutions of nonlinear evolution equations in mathematical physics, *Phys. Lett. A*. **372** (4) (2008) 417-423.

- [25] J.G. Liu, L. Zhou, Y. He, Multiple soliton solutions for the new $(2 + 1)$ -dimensional Korteweg–de Vries equation by multiple exp-function method, *Applied Mathematics Letters*. **80** (2018) 71-78.
- [26] Y. Yakup, Y. Emrullah, A. Abdullahi, A multiple exp-function method for the three model equations of shallow water waves, *Nonlinear Dynamics*. **89** (3) (2017) 2291-2297.
- [27] L.K. Ravi, S. Saha Ray, S. Sahoo, New exact solutions of coupled Boussinesq-Burgers equations by Exp-function method, *Journal of Ocean Engineering and Science*. **2** (1) (2017) 34-46.
- [28] S.A. Li, J.D. Cao, H. Liu, C.D. Huang, Delay-dependent parameters bifurcation in a fractional neural network via geometric methods, *Applied Mathematics and Computation*. **478** (2024) 128812.
- [29] K. Choudhary, B. DeCost, C. Chen, A. Jain, et al., Recent advances and applications of deep learning methods in materials science, *npj Computational Materials*. **8** (1) (2022) 1-26.
- [30] Z.P. Liu, Z.M. Zhang, Z.V. Lei, M. Omura, R.L. Wang, S.C. Gao, Dendritic deep learning for medical segmentation, *IEEE/CAA Journal of Automatica Sinica*. **11** (2024) 803-805.
- [31] K. Hornik, M. Stinchcombe, H. White, Multilayer feedforward networks are universal approximators, *Neural Networks*. **2** (5) (1989) 359-366.
- [32] M. Raissi, P. Perdikaris, G.E. Karniadakis, Physics-informed neural networks: A deep learning framework for solving forward and inverse problems involving nonlinear partial differential equations, *Journal of Computational physics*. **378** (2019) 686-707.
- [33] L. Lu, P.Z. Jin, G.F. Pang, Learning nonlinear operators via DeepONet based on the universal approximation theorem of operators, *Nature Machine Intelligence*. **3** (3) (2021) 218-229.
- [34] S. Wang, H. Wang, P. Perdikaris, Learning the solution operator of parametric partial differential equations with physics-informed DeepONets, *Science advances*. **7** (40) (2021) eabi8605.
- [35] R.F. Zhang, S. Bilige, Bilinear neural network method to obtain the exact analytical solutions of nonlinear partial differential equations and its application to p-gBKP equation, *Nonlinear Dynamics*. **95** (4) (2019) 3041-3048.
- [36] R.F. Zhang, M.C. Li, Bilinear residual network method for solving the exactly explicit solutions of nonlinear evolution equations, *Nonlinear Dynamics*. **108** (1) (2022) 521-531.
- [37] J.G. Liu, W.H. Zhu, Y.K. Wu, G.H. Jin, Application of multivariate bilinear neural network method to fractional partial differential equations, *Results in Physics*. **47** (2023) 106341.

- [38] X.S. Wu, J.G. Liu, Solving the variable coefficient nonlinear partial differential equations based on the bilinear residual network method, *Nonlinear Dynamics*. **112** (10) (2024) 8329-8340.
- [39] Y. Zhu, K.H. Li, C.Y. Huang, et al., Abundant exact solutions of the fractional (3+1)-dimensional Yu–Toda–Sasa–Fukuyama (YTSF) Equation using the Bell Polynomial-based neural network method, *Chaos, Solitons & Fractals*. **196** (2025) 116333.
- [40] E.G. Fan, Extended tanh-function method and its applications to nonlinear equations, *Physics Letters A*. **277** (4) (2000) 212-218.
- [41] S.A. Elwakil, S.K. El-labany, M.A. Zahran, R. Sabry, Modified extended tanh-function method for solving nonlinear partial differential equations, *Physics Letters A*. **299** (2) (2002) 179-188.
- [42] M. Inc, E.G. Fan, Extended tanh-function method for finding travelling wave solutions of some nonlinear partial differential equations, *Zeitschrift fur Naturforschung-Section A Journal of Physical Sciences*. **60** (1-2) (2005) 7-16.
- [43] R.F. Zhang, M.C. Li, M. Albishari, et al., Generalized lump solutions, classical lump solutions and rogue waves of the (2+1)-dimensional Caudrey-Dodd-Gibbon-Kotera-Sawada-like equation, *Applied Mathematics & Computation*. **403** (2021) 126201.
- [44] M.A. Isah, A. Yokus, D. Kaya, Exploring the influence of layer and neuron configurations on Boussinesq equation solutions via a bilinear neural network framework, *Nonlinear Dynamics*. **112** (15) (2024) 13361-13377.
- [45] L.T. Gai, M.H. Xu, R.F. Zhang, N-solitons, lump-stripe solitons with inelastic collisions and new periodic rogue waves of a (2+1)-dimensional extended Sawada-Kotera equation, *Nonlinear Dynamics*. **112**(22) (2024) 20153-20171.
- [46] C.Y. Qin, R.F. Zhang, Y.H. Li, Various exact solutions of the (4+1)-dimensional Boiti–Leon–Manna–Pempinelli-like equation by using bilinear neural network method, *Chaos, Solitons and Fractals*. **187** (2024) 115438.